REVIEWS OF MODERN PHYSICS VOLUME 20, NUMBER 3 JULY, 1948

Energy Partition in Underwater Explosion Phenomena*

A. B. ARONS AND D. R. YENNIE

Woods Hole Oceanographic Institution, Woods Hole, Massachusetts

and

Stevens Institute of Technology, Hoboken, New Jersey

Pressure-time curves, continuous from initial shock wave incidence through the second bubble pulse, are examined in the light of acoustic theory. Calculations of impulse and reversible and irreversible energy flux are made for the various phases of the phenomenon. An estimate has been made of the amount of energy dissipation associated with the propagation of the shock front. A tabulation of the energy partition is included, and it is shown that substantial quantities of energy are radiated or dissipated by mechanisms other than these taken into account in this discussion.

I. INTRODUCTION

1

MOST of the energy released by the detonation of an explosive charge is ultimately imparted to the surrounding medium and becomes distributed among the various phases of succeeding phenomena. It is the purpose of the present investigation to examine the distribution of this energy in underwater explosions, particularly from the point of view of making a complete interpretation of data now available in the form of pressure-time curves.

In general, underwater explosions are characterized by the emission of a shock wave followed by a series of pressure pulses caused by subsequent oscillations of the gas globe containing the products of detonation. A typical pressure-time record is reproduced in Fig. 1.

At the instant following detonation the released energy is present in the form of potential energy of exceedingly high pressure and temperature in the resulting volume of gas. As the gas proceeds to expand it transfers energy to the water. Part of this energy is "radiated" in the sense that it is not stored as reversible potential energy in the water. Rather, it is gradually dissipated by conversion into thermal energy which elevates the temperature of the fluid through which the pressure wave is propagated.

* This investigation was supported under contract with the Navy Department, Bureau of Ordnance. Contribution No. 449 from the Woods Hole Oceanographic Institution.

2

The remainder of the energy transferred to the water is imparted to it as kinetic energy, the water being pushed radially outward against the opposing hydrostatic pressure. The gas globe expansion continues until the energy available to this phase of the motion is stored as potential energy in the water. At this point the gas bubble has attained its maximum radius, and its internal pressure has fallen well below that of the surrounding hydrostatic level. The potential energy now stored in the water is given by

$$E_p = (4/3)\pi A_{M1}{}^3 P_0,$$

where A_{M1} is the maximum bubble radius and P_0 is the absolute hydrostatic pressure. This will be referred to as a "reversible" energy, since it is returned to the gas globe on the succeeding collapsing phase.

The collapse of the bubble and the following expansion are characterized by emission of the first bubble pulse, in which part of the energy E_p is again radiated "acoustically." Thus all the potential energy stored in the water is not returned to the bubble as compressional energy in the gas** at minimum bubble size. An additional

** If the charge is detonated under conditions such that the gas bubble undergoes appreciable migration because of the influence of gravity or boundary surfaces, a substantial part of E_p will be imparted irreversibly to vertical motion of the water. The condition principally considered in this report is that in which the bubble migration is negligibly small. This, however, has no bearing on considerations

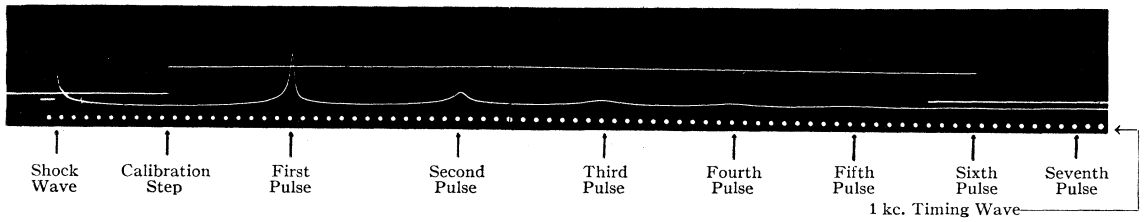

FIG. 1. Pressure-time record showing shock wave and bubble pulses. Charge: 0.505-lb. TNT; gauge dist: 2.25 ft.; depth: 500 ft.

loss occurs on re-expansion, resulting in a value A_{M2} (for the second maximum in the bubble radius) considerably smaller than A_{M1}.

3

In addition to the energy observed in waves of compression and in reversible interchange between the gas globe and the water, energy is also being continually dissipated because of various other factors such as:

(i) radiation and conduction from gas globe,
(ii) viscous loss in the water,
(iii) turbulent loss in the water.

4

An observer at a fixed point (radial distance R from the center of the charge) would see a "flow" of energy past his point in the positive or negative direction of R, depending upon the phase of the explosion phenomenon. Piezoelectric gauge measurements provide a record of pressure *vs.* time at just such a point of observation. In order to investigate the energy flux, it is necessary to have a relation between energy and the variables pressure and time. These relationships are developed in the following chapter.

The experimental results to be quoted subsequently were all obtained from measurements on TNT.

II. GENERAL EXPRESSIONS FOR ENERGY FLUX

5

In this report the energy flux will be defined as the amount of energy that passes through a unit area of surface during a given time interval. In the case of spherical symmetry this energy flux will be uniform over the surface of a sphere, and the total flow of energy through the spherical surface will be given by:

$$E=4\pi R^2F. \tag{1}$$

The symbol E will be used to designate the total energy flow through the surface, and a component of the total will be indicated by attaching a suitable subscript. The symbol F will be used in a similar way to represent the energy flux.

In general, the energy flux will be found to consist of a number of components varying inversely as some power of the radius:

$$F=F_1/R^{n_1}+F_2/R^{n_2}+F_3/R^{n_3}+\cdots \text{ etc.} \tag{2}$$

If the value of an exponent n happens to be 2, Eq. (1) shows that the total energy flow, E, corresponding to that term will be the same at all radii and therefore the energy will be radiated away to infinity. If the value of n is greater than 2, the total energy flow will be smaller at larger radii, indicating that some energy has been left behind in the water. In some cases the energy left in the water is in the form of kinetic energy or other undissipated forms and therefore should be returned ultimately to the gas globe. In other cases it represents an energy which has been dissipated irreversibly and goes into heating of the water.

6

The general expression for what might be termed the "useful" total energy flow through a sphere of radius R relative to the center of the explosive charge is given by the following time integral:

$$E=4\pi R^2\int_0^{t_1}\left(\frac{\Delta p}{\rho}+\tfrac{1}{2}u^2+\Delta\eta\right)\rho u dt, \tag{3}$$

pertaining to events up to the first bubble maximum, since migration never becomes appreciable until the phase of bubble collapse.

where t = time measured from instant of incidence of the pressure wave, t_1 = arbitrary upper limit of integration, Δp = excess pressure $(p-P_0)$, a function of time, P_0 = absolute hydrostatic pressure level at point of detonation, u = particle velocity relative to the unperturbed fluid, ρ = density of the fluid at time t, $\Delta\eta$ = increase in internal energy of a unit mass of fluid relative to the initially unperturbed state.

The term in Δp represents a compressional energy capable of doing work against the fluid external to the sphere through which it passes. The second term represents the kinetic energy of the mass of fluid moving past the point of observation, while the third term in $\Delta\eta$ represents the increment of internal energy of this mass. It will be shown that at values of R which are large relative to the initial charge radius, the last two terms are both very small compared to the term in Δp.

7

The type of experimental data available for making an analysis of the energy flux consists mainly of pressure-time curves recorded by means of piezoelectric gauges.[1]

Such data have previously been available for the shock wave to times of the order of 10θ, where θ is the time constant of the initially exponential shock-wave decay. Additional data have recently been obtained from bubble pulse measurements,[2] making it possible to extend the pressure-time curve from 10θ through the second bubble pulse.

If u in Eq. (3) can be expressed in terms of the variables Δp and t, it becomes possible to evaluate energy transfer from the primary pressure-time data. A rigorous development would involve the exact solution of the hydrodynamical equations of motion. Such a solution would involve exceedingly laborious and complicated numerical integrations which are impractical except in a very few special cases.

Fortunately the compressibility of water is sufficiently low to make the so-called acoustic approximation useful (and probably adequate) for the treatment of pressure-time data in the region normally accessible to experimental measurement.

8

The acoustic approximation in a case of spherical symmetry yields the following relationship for the particle velocity, u:[3]

$$u=\frac{\Delta p}{\rho_0 C_0}+\frac{1}{\rho_0 R}\int_0^t \Delta p\,dt, \tag{4}$$

where

ρ_0 = the density of the unperturbed fluid,
$C_0=(\partial P/\partial\rho_0)_{s_0}^{\frac{1}{2}}$, the velocity of sound in the fluid.

The second term on the right-hand side of Eq. (4) is frequently referred to as the afterflow term in the particle velocity.

Combining Eqs. (4) and (3) we find

$$E=4\pi R^2\left\{\int_0^{t_1}\left(\frac{\Delta p}{\rho}+\tfrac{1}{2}u^2+\Delta\eta\right)\frac{\rho\Delta p}{\rho_0 C_0}dt + \int_0^{t_1}\left[\frac{((\Delta p/\rho)+\frac{1}{2}u^2+\Delta\eta)\rho}{\rho_0 R}\int_0^t \Delta p\,dt\right]dt\right\}. \tag{5}$$

The sum $(\frac{1}{2}u^2+\Delta\eta)$ is small relative to $\Delta p/\rho$, as will be shown in Section 10; at low values of Δp it can be neglected entirely. A correction is justified at high values of Δp, but only the first term in Eq. (5) requires this correction since the second term is initially zero and does not acquire appreciable value until after the elapse of a certain amount of time, during which the pressure is decaying very rapidly.

The Rankine-Hugoniot conditions*** afford relationships for u, U, and $\Delta\eta$ in terms of Δp and the change in density across a shock front. (U represents the velocity of propagation of the shock.)

$\Delta\eta$ and u in the first term of Eq. (5) are then replaced by the appropriate Hugoniot relations

[1] J. S. Coles, OSRD Report No. 6240.
[2] A. B. Arons, J. P. Slifko, and A. Carter, J. Acous. Soc. Am. **20**, 271 (1948), and A. B. Arons, *ibid.* **20**, 277 (1948).

[3] H. Lamb, *Hydrodynamics* (University Press, Cambridge, 1932), p. 490.

*** The Rankine-Hugoniot conditions are obtained by application of the laws of conservation of mass, momentum, and energy at the shock front (see reference 3). These conditions are:

$$U=v_0((p-P_0)/(v_0-v))^{\frac{1}{2}},$$
$$u=((p-P_0)(v_0-v))^{\frac{1}{2}},$$
$$\Delta\eta=\tfrac{1}{2}(P_0+p)(v_0-v),$$
$$\Delta H=\Delta\eta+\Delta(pv)=\tfrac{1}{2}(p-P_0)(v_0+v).$$

and C_0 is replaced by the propagation velocity U. This is equivalent to treating the fluid at time t behind the shock front as though it had just passed from its unperturbed state through a shock front of corresponding amplitude Δp, i.e., directly along a Hugoniot curve from 0 to Δp. Strictly speaking this is not correct, since the particle of fluid under consideration has actually passed through a shock front of greater amplitude at a preceding time and has returned to the pressure Δp along an adiabatic. Also neglected is the effect of spherical divergence on the particle velocity, u. However, the above substitution is introduced as a first approximation, and since the correction is quite small for all practical cases, the approximation is probably adequate.

Making the substitution discussed above in the first term of Eq. (5) and neglecting $\frac{1}{2}u^2$ and $\Delta\eta$ in the second term, one obtains, after algebraic manipulation:

$$E=\frac{4\pi R^2}{\rho_0}\left\{\int_0^{t_1}\frac{(\Delta p)^2}{U-\dfrac{\Delta p}{\rho_0 U}}dt+\frac{1}{R}\int_0^{t_1}\left[\Delta p\int_0^t\Delta p dt\right]dt\right\}^{\dagger} \quad (6)$$

For comparison, it is convenient to state the result yielded by Eq. (5) if $\frac{1}{2}u^2$ and $\Delta\eta$ are neglected throughout and C_0 is not substituted by U:

$$E=4\pi R^2\left\{\frac{1}{\rho_0 C_0}\int_0^{t_1}(\Delta p)^2dt+\frac{1}{\rho_0 R}\int_0^{t_1}\left[\Delta p\int_0^t\Delta p dt\right]dt\right\}. \quad (7)$$

It will be shown in Section 10 that Eq. (6) differs from Eq. (7) only in that the first term contains a correction factor which does not depart from unity by more than a few percent at pressures as high as 20- or 30-thousand pounds per square inch.

† Note that the second integral of Eq. (6) may also be written in the form:

$$\frac{1}{2R}\left[\int_0^{t_1}\Delta p dt\right]^2,$$

this form being more useful for purposes of computation.

In acoustic theory Δp varies inversely as R, the distance from the origin. Inspection of Eq. (7) in the light of Eq. (2) therefore indicates that the first term on the right-hand side represents principally "radiated" energy associated with what will be termed the "irreversible energy flux," while the second term represents energy stored reversibly in the region covered by the shock wave. It should be noted that the small contributions made by $\frac{1}{2}u^2$ and $\Delta\eta$ to the first term are also reversible.

III. THE FIRST TERM FOR THE ENERGY FLUX IN THE SHOCK WAVE

To complete the development of expressions necessary for the interpretation of pressure-time data, we return to that part of the energy flux as given by the first term of Eq. (6):

$$F_1=\frac{1}{\rho_0}\int_0^{t_1}\frac{(\Delta p)^2}{U-(\Delta p/\rho_0 U)}dt. \quad (8)$$

The Rankine-Hugoniot conditions give a relation for U in terms of Δp at a shock front:

$$U=v_0(\Delta P_s/v_0-v)^{\frac{1}{2}}, \quad (9)$$

where ΔP_s is the excess pressure at the shock front and v_0 and v are the specific volumes of the fluid ahead and behind the shock front, respectively.

Combination of Eq. (9) with certain thermodynamic relations and with equation of state data[4] makes it possible to calculate U for corresponding arbitrary values of ΔP_s. Such calculations have been made for sea water at quite closely spaced values of ΔP_s, and the results can be represented empirically by the following approximate fit:

$$U=C_0[1+5.6\times10^{-6}\Delta P_s-17\times10^{-12}(\Delta P_s)^2], \quad (10)$$

where the excess pressure is expressed in lb./in.^{2}. For the purpose of obtaining a first-order correction to the energy flux, the propagation velocity may be represented approximately by the following linear relation:

$$U=C_0[1+\alpha\Delta P_s],\qquad U=C_0[1+5.3\times10^{-6}\Delta P_s]. \quad (11)$$

[4] J. M. Richardson, A. B. Arons, and R. R. Halverson, J. Chem. Phys. **15**, 785 (1947).

Equation (10) fits the results of reference (4) quite closely from zero to 60,000 p.s.i., while Eq. (11) represents a rough average fit of a straight line in the region from zero to 40,000 p.s.i. Equation (11) falls slightly below the true values at low and somewhat above at high pressures.

Inserting Eq. (11) into Eq. (8), and carrying the result to first-order terms, the following expression is obtained:

$$F_1=\frac{1}{\rho_0 C_0}\int_0^{t_1}(\Delta p)^2\left[1-\left(\alpha-\frac{1}{\kappa}\right)\Delta p\right]dt, \quad (12)$$

where $\kappa=\rho_0 C_0^2$.

The same expression may be derived by applying first-order corrections directly to the general expression given in Eq. (5):

$$F_1=\int_0^{t_1}\left(\frac{\Delta p}{\rho}+\tfrac{1}{2}u^2+\Delta\eta\right)\rho u dt, \quad (13)$$

where u is given by the Rankine-Hugoniot conditions

$$u=(\Delta p/\rho_0 U),$$

and the internal energy increment, $\Delta\eta$, is approximately the compressional energy of the fluid:

$$\Delta\eta=\tfrac{1}{2}(\Delta p)^2/\kappa\rho_0, \quad (14)$$

κ being the bulk modulus. The kinetic energy per unit mass is

$$\tfrac{1}{2}u^2=\tfrac{1}{2}(\Delta p)^2/\rho_0^2U^2\approx\tfrac{1}{2}(\Delta p)^2/\rho_0^2C_0^2 =\tfrac{1}{2}(\Delta p)^2/\rho_0\kappa=\Delta\eta. \quad (15)$$

Equation (12) is verified by substituting these relations in Eq. (13) and carrying the results to first-order terms.

In its present form, Eq. (12) is unwieldy because it requires integrations of both $(\Delta p)^2$ and $(\Delta p)^3$. The term in $(\Delta p)^3$, however, introduces only a small correction, and it is convenient to represent the average value of this correction in terms of one convenient parameter, such as the peak pressure of the shock wave. To do this, it is assumed that the shock-wave pressure varies exponentially with time.

$$\Delta p=P_m\epsilon^{-t/\theta}.$$

Although this is not a correct representation of the whole wave, it is true for times up to $t=\theta$, from which region most of the correction to the energy flux actually stems. Therefore, applying this approximation

$$\int_0^\infty(\Delta p)^2dt=\frac{P_m^2\theta}{2},$$

$$\int_0^\infty(\Delta p)^3dt=\frac{P_m^3\theta}{3}=\tfrac{2}{3}P_m\int_0^\infty(\Delta p)^2dt.$$

The first energy flux term then becomes

$$F_1=\frac{1}{\rho_0 C_0}\left[1-\tfrac{2}{3}\left(\alpha-\frac{1}{\kappa}\right)P_m\right]\int_0^{t_1}(\Delta p)^2dt. \quad (16)$$

The correction represented by the second term in the bracket is small (the order of a few percent), so that even though the correction itself might be subject to a large error because of the crudeness of various approximations, the final result for energy flux should not be greatly in error. For P_m in lb./in.^{2}, and F_1 in in. lb./in.^{2}, Eq. (16) may be written

$$F_1=\frac{1}{\rho_0 C_0}[1-1.6\times10^{-6}P_m]\int_0^{t_1}(\Delta p)^2dt. \quad (17)$$

Equation (17) is based on U as given by Eq. (11). This equation can now be used in the computation of the energy flux given by the first term of Eq. (5).

This approximation can easily be carried to second-order terms, although for most applications this is an unnecessary refinement. The result to second order is

$$F_1=\frac{1}{\rho_0 C_0}[1-1.8\times10^{-6}P_m+4\times10^{-12}P_m^2]\times\int_0^{t_1}(\Delta p)^2dt. \quad (18)$$

Equation (18) is based on U as given by Eq. (10).

If pressures are expressed in lb./in.^{2} and time in seconds, F_1 is obtained in in. lb./in.^{2} by using

$$\rho_0 C_0=5.58+0.0065T, \quad (19)$$

where T is temperature of the water in degrees centigrade.

The quantity $\rho_0 C_0$ is commonly called the acoustic impedance of the medium. Equation (19) applies specifically to sea water having a salinity of 32 parts per thousand.

10

It is now possible to investigate the relative magnitude of the terms for internal and kinetic energy in Eq. (3). The part of the energy flux given by these terms is

$$F_c = \int_0^{t_1} (\tfrac{1}{2}\rho u^2 + \rho\Delta\eta) u dt. \qquad (20)$$

From Eqs. (14) and (15)

$$\tfrac{1}{2}\rho u^2 = \rho\Delta\eta = \tfrac{1}{2}(\Delta p)^2/\kappa, \qquad (14), (15)$$

and the particle velocity is given by

$$u = \Delta p/\rho_0 C_0,$$

approximately.

Using the exponential approximation for the pressure *versus* time relation, the part of energy flux given by Eq. (20) becomes

$$F_c = \frac{1}{\rho_0 C_0}\left(\frac{2}{3}\frac{P_m}{\kappa}\right)\int_0^{t_1} (\Delta p)^2 dt$$

$$= \frac{1}{\rho_0 C_0}(2\times 10^{-6} P_m)\int_0^{t} (\Delta p)^2 dt, \qquad (21)$$

where pressures are in lb./in.^{2} and the energy flux is in in. lb./in.^{2}. The term $(2\times 10^{-6} P_m)$ represents a fractional part of the total energy flux given by Eq. (17). The contribution of the kinetic and internal energy terms to the flux F_1 is, therefore,

$$\frac{F_c}{F_1} = \frac{2\times 10^{-6} P_m}{1 - 1.8\times 10^{-6} P_m}\times 100 \text{ percent}$$

or approximately

$$(2\times 10^{-4} P_m) \text{ percent}. \qquad (22)$$

At the highest pressure levels so far investigated (*ca.* 30,000 to 40,000 lb./in.^{2}) this contribution is of the order of a few percent. For pressures below 10,000 lb./in.^{2} the contributions of the kinetic and internal energy terms are negligibly small.

IV. ENERGY DISSIPATION AT THE SHOCK FRONT

11

Acoustic theory, which does not admit dissipative effects, predicts that the pressure in a spherically divergent wave will decay as the inverse first power of the radial distance. It would naturally be expected that a finite amplitude wave should decay somewhat more rapidly, and this fact has been confirmed by experimental pressure-distance curves.

As noted in Section 5, a decay of this type implies that some energy is being left behind as thermal energy in the water through which the wave has passed. Most of this dissipation can probably be ascribed to the irreversible thermodynamic process occurring at the shock front.

As an element of fluid passes through the shock front, it undergoes a sudden non-isentropic compression, the final state being determined by the Rankine-Hugoniot conditions.[4] When the pressure later drops to the hydrostatic level, it is found that the element of fluid has suffered a net increase of enthalpy (and entropy). This increase of enthalpy, which depends on the magnitude of the pressure at the shock front, is known as the dissipated enthalpy increment and will be designated by the symbol h.

The dissipated enthalpy increment is approximately proportional to the cube of the shock-wave pressure for low and moderate pressures, the limiting law for low pressures being given by[5]

$$h = (1/12)(\partial^2 v/\partial P^2)_s (\Delta P_s)^3. \qquad (23)$$

Using the Ekman equation of state[4] for sea water and applying Eq. (23), it is found that

$$h = 1.52\times 10^{-10}(\Delta P_s)^3, \qquad (24)$$

where h is in in.-lb./lb. and ΔP_s is in lb./in.^{2}. Equation (24) holds quite well for pressures up to 5000 lb./in.^{2}.

12

For higher pressures a modified adiabatic Tait equation of state has been used:[4]

$$P = B(S)[(v_1/v)^n - 1], \qquad (25)$$

[5] J. G. Kirkwood and H. Bethe; J. G. Kirkwood and E. Montroll, OSRD Reports No. 588 and 676.

where $n=7.15$ and $B(S)=44{,}400$ lb./in.^{2}. v_1 is the final specific volume after return to hydrostatic pressure, and v is the specific volume immediately after the passage of the shock wave. This equation of state leads to the following formula[4] for the dissipated enthalpy increment:

$$h=\frac{Bv_1}{2}\left[\left(\frac{v_1}{v}\right)^n-\frac{n+1}{n-1}\left\{\left(\frac{v_1}{v}\right)^{n-1}-1\right\}-\frac{v}{v_1}\right]-\frac{B(v_1-v_0)}{2}\left[\left(\frac{v_1}{v}\right)^n-1\right]. \quad (26)$$

The term v_0 appearing here is the specific volume of the fluid before the arrival of the shock front. The last term on the right is relatively small and may be neglected for shock pressures under 40,000 lb./in.^{2}.

Figure 2 shows a plot of h as a function of the shock pressure, as computed from Eq. (26).

13

In a spherical wave the energy dissipated between two spherical shells is given by

$$E_D=4\pi\rho_0\int_{R_1}^{R_2}R^2h(\Delta P_s)dR, \quad (27)$$

where $h(\Delta P_s)$ is the dissipated enthalpy increment at pressure ΔP_s, and ΔP_s is the excess shock pressure at distance R from the origin.

This integral can be evaluated in the low pressure region by use of Eq. (25) and at higher pressure by use of Eq. (26), providing experimental data are available, giving ΔP_s as a function of the radial distance R.

Reliable pressure-distance data, based on piezoelectric measurements, are available up to pressures of 20 to 30 thousand lb./in.^{2}. A few experimental points based upon measurement of spray dome velocities are available at higher pressures, but values for the region between the surface of the charge and the 30,000 lb./in.^{2} pressure level must be based principally upon theoretical calculations such as those of Kirkwood, Bethe *et al.*,[5] or Brinkely and Kirkwood.[6]

Available estimates of the pressure in the water at the surface of the charge range from 30 to 50 kilobars. The calculations cited[5, 6] both lead to values close to 36 kilobars.

In Fig. 3 the pressure-radius similarity curve for TNT is shown extrapolated back to two arbitrary values at the charge surface. The value of 36 kilobars or 520,000 lb./in.^{2} is considered to be the order of magnitude of the actual peak pressure. The similarity curve extrapolated to 1,000,000 lb./in.^{2} is given for purposes of comparison as a possible upper limit of error. Isolated experimental values from dome velocity measurements are plotted on the same figure.

Using values from Fig. 3, the integrand of Eq. (27) is shown plotted in Fig. 4. For the solid curve of this figure the empirical relation $x^2h=1230x^{-1.23}$ (where $x=R/W^{\frac{1}{3}}$) satisfactorily represents the integrand between the limits of $x=0.136$ and $x=10$. The dashed curve represents an upper limit to the integrand based on a peak pressure of 1,000,000 lb./in.^{2} at the charge. This curve is drawn to indicate the possible extent of the error in calculating the energy dissipation.

From the empirical relation given above, the energy dissipated between any two spherical surfaces may be readily calculated:

$$\frac{E_D}{W}=4\pi\rho_0\int_{x_1}^{x_2}1230x^{-1.23}dx$$
$$=4{,}300{,}000[(W^{\frac{1}{3}}/R_1)^{0.23}-(W^{\frac{1}{3}}/R_2)^{0.23}]\ \frac{\text{in.-lb.}}{\text{lb. chg.}}, \quad (28)$$

where W is charge weight in. lb. and R is in ft.

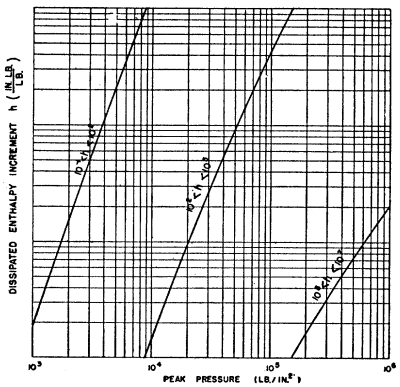

FIG. 2. Dissipated enthalpy increment, h, *versus* shock front pressure, ΔP_s.

[6] S. R. Brinkely and J. G. Kirkwood, Phys. Rev. **71**, 606 (1947).

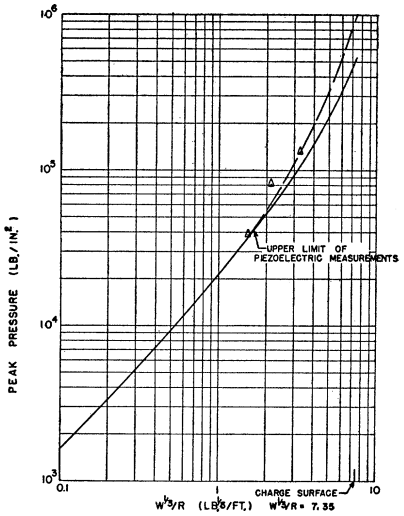

FIG. 3. Peak pressure similarity curve for TNT. Legend: △ isolated experimental points based on measurement of spray dome velocity. ——— experimental curve based on piezoelectric measurements, extrapolated to a theoretical value at the charge surface based upon the results of reference 5, 6. – – – – similarity curve arbitrarily extrapolated to a value of 10^6 lb./in.^{2} at the charge surface.

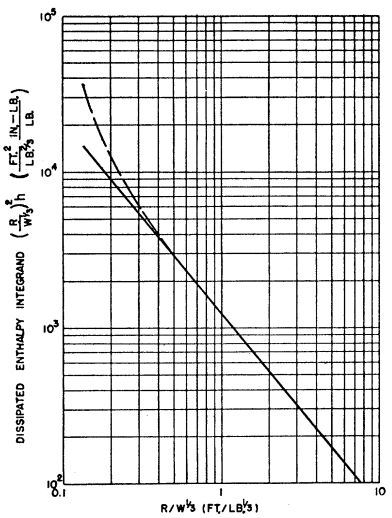

FIG. 4. Dissipated enthalpy integrand, $(R/W^{\frac{1}{3}})^2 h$, *versus* $R/W^{\frac{1}{3}}$ for TNT. Legend: ——— based on solid curve, Fig. 3. – – – – based on dashed curve, Fig. 3.

As an example, the amount of energy dissipated between the charge surface, $(W^{\frac{1}{3}}/R) = 7.35$, and a radius given by $R = W^{\frac{1}{3}}/0.352$ is approximately 3,400,000 in. lb. per pound of charge or 200 cal./g of charge.

A calculation based on the dashed curve of Fig. 4 for the same limits of integration would yield roughly 25 percent additional dissipated energy. The actual error is probably smaller than this, but the above value is an indication, at least, of the uncertainties involved in the assumption of the form of the pressure-radius curve in the region very close to the charge.

It must be remembered that an additional error, the magnitude of which cannot be estimated, is present because of uncertainty with respect to the equation of state data in the high pressure region. The equations used are based on extrapolation of experimental data[4] from pressures of 10 kilobars, and at high pressures actually imply applicability to metastable liquid water in the ice VII region.

14

It is now possible to compare the measured shock-wave energy flux at different radii with the loss caused by dissipation. Unfortunately, there is considerable scatter in the shock-wave data available, so that it is hard to state precisely what the energy flux is at a given radius. As a result, the total energy flow through a surface is known only to within about 5 to 10 percent, and although the total flow at a given radius may be known to within these limits, the experimentally measured dissipation, which is given by the small difference between flow at each of two radii, will be very appreciably in error.

To illustrate this, for TNT the flux at $W^{\frac{1}{3}}/R = 1$ is 2700 ± 250 in. lb./in.^{2} lb.$^{\frac{1}{3}}$, and at $W^{\frac{1}{3}}/R = 0.1$ it is 20.5 ± 1.5 in. lb./in.^{2} lb.$^{\frac{1}{3}}$. The total energy flow at $W^{\frac{1}{3}}/R = 1$ is then $4{,}900{,}000 \pm 450{,}000$ in. lb./lb. and at $W^{\frac{1}{3}}/R = 0.1$ it is $3{,}700{,}000 \pm 270{,}000$ in. lb./lb. The energy dissipated in the interval $W^{\frac{1}{3}}/R = 1$ to 0.1 calculated from these figures is $1{,}200{,}000 \pm 720{,}000$ in. lb./lb. The large uncertainty in the dissipated energy is immediately apparent. (These values are obtained from data taken at Woods Hole by J. S. Coles and his coworkers.)

By the use of Eq. (28), the energy loss resulting from dissipation between $W^{\frac{1}{3}}/R = 1$ and $W^{\frac{1}{3}}/R = 0.1$ would be 1,760,000 in. lb./lb. This value is to be compared with that of $1{,}200{,}000 \pm 720{,}000$ in. lb./lb. obtained above from the Woods Hole data. It will be noted that the two results agree within the limit of error of the experimental measurement. The calculated value,

based on a knowledge of the somewhat more accurate pressure-distance curve, is probably the better of the two.

V. IMPULSE AND ENERGY FLUX ASSOCIATED WITH THE SHOCK WAVE

15

The general character of the pressure wave emitted by an underwater explosion is illustrated by the oscilloscope trace reproduced in Fig. 1. The first portion is generally referred to as the shock wave, and this in turn is succeeded by the first, second, etc., bubble pulses. The pressure-time record is continuous, and naturally there is no sharply defined demarcation between the various portions of the wave. For convenience, an arbitrary demarcation will be introduced for the purposes of this report.

The shock wave will be defined as the portion of the wave lying between the shock front ($t=0$) and the first bubble maximum ($t=t_{M1}$) which occurs at the pressure minimum lying halfway between the shock front and the peak of the first bubble pulse. The first bubble pulse will be defined as the portion of the wave lying between the times of first and second bubble maxima (i.e., between $t=t_{M1}$ and $t=t_{M2}$), etc., for the succeeding pulses.

Usually, shock-wave pressure-time recording is carried only to times of the order of 10θ, where θ is the time constant of the initial exponential decay. Recently, a series of deep water measurements[2] has provided data making it possible to construct average or composite curves out to time t_{M1} as defined above. These curves are based on measurements with 0.50-, 2.50-, and 12.0-lb. charges of TNT at depths of 250 and 500 ft. Gauges were placed at such distances as to keep the value of $W^{\frac{1}{3}}/R$ constant at 0.352 for each charge size. The curves are shown in Figs. 5, 6, and 7.

16

The impulse delivered up to any time t is defined by

$$I=\int_0^t \Delta p dt. \tag{29}$$

The shock wave has an initial positive phase of relatively short duration and high amplitude followed by a long negative phase of low amplitude. The positive portion of the impulse is of principal interest as far as damage considerations are involved.

As the integration is carried to t_{M1}, the value of the integral becomes very small and in an incompressive system would become zero. In a compressive fluid the integral has a small positive residual at t_{M1}, as indicated in the following.

At t_{M1} the bubble has attained maximum radius, and the particle velocity at its surface is zero. In the acoustic approximation the particle velocity as a function of time at a point in the fluid is given by

$$u=\frac{\Delta p}{\rho_0 C_0}+\frac{1}{\rho_0 R}\int_0^t \Delta p dt. \tag{30}$$

If we make an observation at $R=A_{M1}$, where A_{M1} is the maximum bubble radius, then at

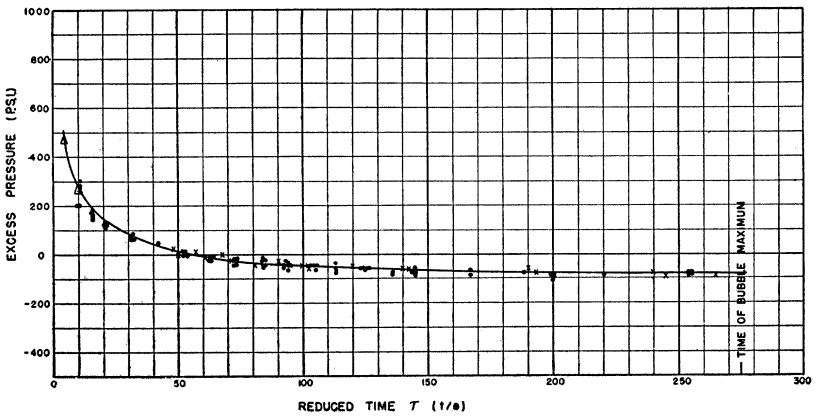

FIG. 5. Composite pressure-time curve for tail of shock wave. Explosive: TNT; charge depth: 250 ft.; distance from center of charge: $R=W^{\frac{1}{3}}/0.352$. Legend: θ time constant of initial shock wave decay, ●, × 0.5-lb. and 2.5-lb. charges from measurements of reference 2. Δ Points from shock-wave composites obtained by J. S. Coles *et al.*, Woods Hole.

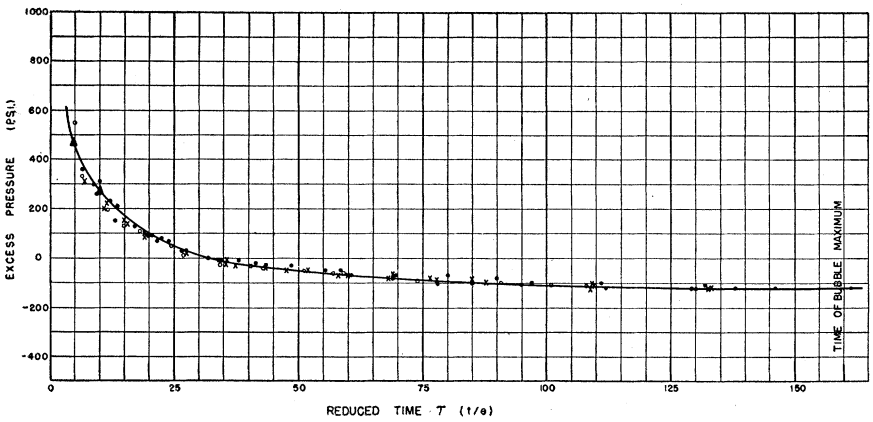

FIG. 6. Composite pressure-time curve for tail of shock wave. Explosive: TNT; charge depth: 500 ft.; distance from center of charge: $R=W^{\frac{1}{3}}/0.352$. Legend: θ time constant of initial shock-wave decay. ●, ×, ⊙ 0.5-, 2.5-, and 12.0-lb. charges based on measurements of reference 2. Δ Points from shock-wave composites obtained by J. S. Coles *et al.*, Woods Hole.

$t=t_{M1}$, $u_{M1}=0$ and from Eq. (30)

$$I_{M1}=\int_0^{t_{M1}}\Delta p dt=-\frac{A_{M1}\Delta p}{C_0}. \tag{31}$$

Since Δp is negative in this region, I_{M1} is inherently positive. Its magnitude is very small compared to that of the total positive or negative impulse.

17

Combining Eqs. (6) and (17), the complete expression for total energy flow to time t becomes

$$E=\frac{4\pi R^2}{\rho_0 C_0}\left[(1-1.6\times10^{-6}P_m)\int_0^t(\Delta p)^2dt+\frac{C_0}{2R}\left(\int_0^t\Delta p dt\right)^2\right]. \tag{32}$$

As previously indicated, the first term in the bracket increases monotonically with increasing time of integration and represents energy radiated acoustically, while the second or afterflow term represents energy which is stored reversibly in the water and returned at intervals to the gas bubble. This term attains a maximum at time t corresponding to the end of the positive phase and then decreases, becoming virtually zero at $t=t_{M1}$ since it involves the squaring of the small residual impulse given by Eq. (31). In the later stages of the positive phase at distances fairly close to the charge, the afterflow term predominates over the irreversible term.

Although in the limit of low pressures the afterflow term represents the contribution of essentially incompressive flow consequent upon the bubble expansion, it cannot be regarded as a purely incompressive term throughout the integration. Incompressive and compressive effects are not dissociable in the acoustic approximation, and in the region just behind the shock front the afterflow term represents principally a compressive contribution due to the radial divergence of the flow initiated by passage of the wave of compression.

18

Figures 5, 6, and 7 are composite pressure-time curves for TNT at the depths of 250 and 500 ft. and at a distance from the charge given by $W^{\frac{1}{3}}/R=0.352$. Several charge sizes have been plotted on the same curve by scaling the time in terms of θ, the time constant of initial shock wave decay which is given by††

$$\theta=0.060W^{\frac{1}{3}}(W^{\frac{1}{3}}/R)^{-0.18}$$
$$=0.0725W^{\frac{1}{3}}\text{ millisec. at }W^{\frac{1}{3}}/R=0.352. \tag{33}$$

Using this scale factor, the reduced time τ is defined by

$$\tau=t/\theta. \tag{34}$$

τ is, of course, a dimensionless quantity. Any other scale factor proportional to $W^{\frac{1}{3}}$, such as the bubble period at the given depth, might equally well have been used.

From the pressure-time curves in Figs. 5, 6, and 7, certain quantities (listed below) have been

†† Equation (33) is an empirical fit of TNT data obtained at Woods Hole by J. S. Coles *et al.*

computed and plotted in Figs. 8, 9, and 10. Figure 8 shows curves for the initial positive phase, i.e., up to the time at which the excess pressure at the point of observation becomes zero following the arrival of the shock wave. This figure is for a charge depth of 500 ft. only, but a similar one for a depth of 250 ft. would not be very different. Figures 9 and 10 show the same curves extended to the time of first bubble maximum for depths of 250 ft. and 500 ft., respectively. They are essentially the same in form, the principal differences being due to the longer negative phase and smaller negative pressure at the 250-ft. depth. The functions plotted in Figs. 8, 9, and 10 are:

a. Irreversible energy flux, given by

$$F_1=\frac{1}{\rho_0 C_0}[1-1.6\times10^{-6}P_m]\int_0^t(\Delta p)^2dt. \quad (32a)$$

b. Afterflow: the afterflow energy flux should, according to the criterion of Section 5, average out to zero because it does not represent a radiated or an irreversibly stored energy. Afterflow energy flux is given by

$$F_A=\frac{1}{2\rho_0 R}\left(\int_0^t \Delta p dt\right)^2=\frac{I^2}{2\rho_0 R}. \quad (32b)$$

Since the total impulse up to $t=t_{M1}$ is very small, the total afterflow energy up to this time is also very small. Physically what has happened is that the afterflow velocity was always outward, while the excess pressure was first positive, then negative. At one time the afterflow was with the pressure, later against it so that the total work done because of the motion has a net value that is very small, while each of its positive and negative components are large in magnitude.

c. Impulse: the impulse is defined by

$$I=\int_0^t \Delta p dt. \quad (29)$$

d. Particle velocity: the total particle velocity is given by

$$u=\frac{\Delta p}{\rho_0 C_0}+\frac{1}{\rho_0 R}\int_0^t \Delta p dt. \quad (30)$$

Separate curves for each component of the particle velocity have not been plotted, since their form may be obtained directly from the pressure-time and impulse-time curves. The form of the total particle velocity curve will change with the distance from the charge, since the two components vary as the first and second powers of the radius, respectively. The curves shown apply to the specific case where $R=W^{\frac{1}{3}}/0.352$.

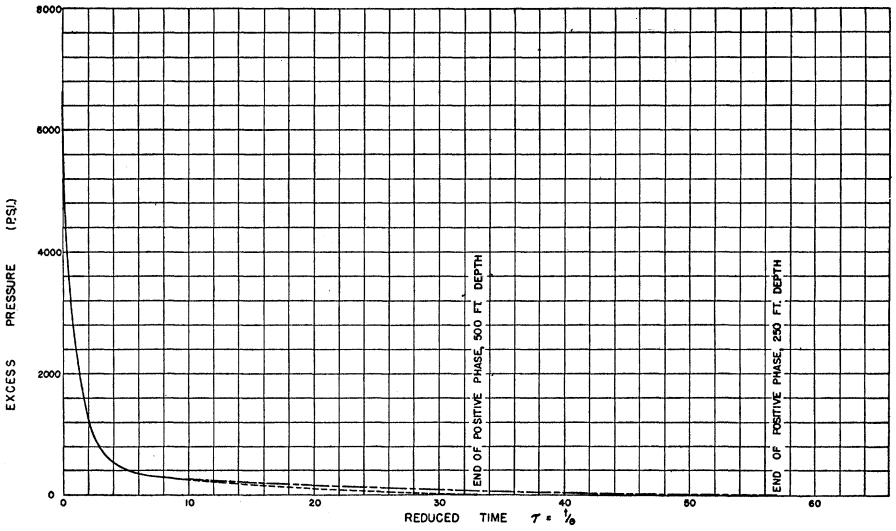

FIG. 7. Composite pressure-time curve for entire shock wave. Explosive: TNT; distance from center of charge: $R=W^{\frac{1}{3}}/0.352$. Legend: θ time constant of initial shock wave decay. ——— initial portion of shock wave from measurements by J. S. Coles *et al.*, Woods Hole. — · — tail of curve from Fig. 5, 250-ft. depth. – – – – tail of curve from Fig. 6, 500-ft. depth.

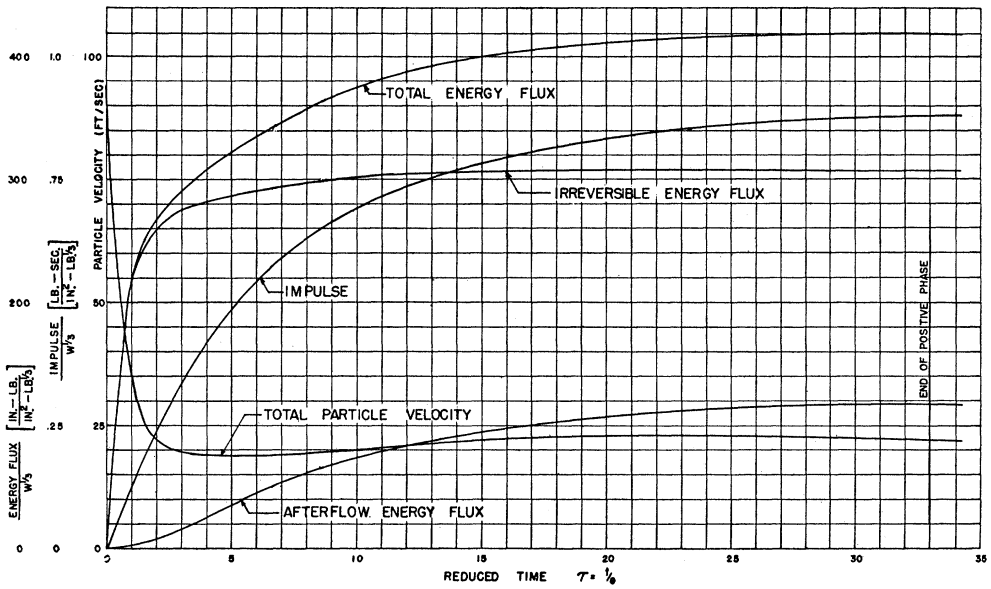

FIG. 8. Energy flux, impulse, and total particle velocity *versus* time for initial positive pressure phase of shock wave. Explosive: TNT; charge depth: 500 ft.; distance from center of charge: $R=W^{\frac{1}{3}}/0.352$. θ=time constant of initial shock-wave decay.

The total volume flow through a spherical surface may be expressed as

$$\Delta V=4\pi R^2\int_0^t u dt.$$

In the case under consideration, the total volume flow up to the time of bubble maximum is

$$\Delta V=4\pi R^2\int_0^{t_{M1}}\frac{\Delta p}{\rho_0 C_0}dt + 4\pi R^2\int_0^{t_{M1}}\left[\int_0^t\frac{\Delta p}{\rho_0 R}dt\right]dt,$$

and since the first term on the right is very small,

$$\Delta V\approx\frac{4\pi R}{\rho_0}\int_0^{t_{M1}}\left[\int_0^t\Delta p dt\right]dt. \qquad (35)$$

Since ΔV is nearly independent of the radius, Eq. (35) should give us the total flow through the surface at the maximum bubble radius, i.e., the volume of the bubble at t_{M1}. This volume may also be calculated independently from experimental knowledge of the maximum radius.

From high speed photographic work carried out at Woods Hole by J. C. Decius and E. Swift, the following empirical equation relating maximum bubble radius to charge size and depth has been obtained:

$$A_{M1}=J_1(W/Z_0)^{\frac{1}{3}}. \qquad (36)$$

A_{M1} is maximum bubble radius in feet, W is charge weight in pounds, Z_0 is the total hydrostatic head in feet (depth +33 ft.), and J_1 is a nearly constant factor which has a value of 12.6 for TNT over the range of depths under consideration.

At a depth of 500 ft. Eq. (35), utilizing the pressure-time curve of Fig. 6, gives a volume of 17 cu. ft. per lb. of explosive, while Eq. (36) gives 15.7 cu. ft. per lb. At 250 ft. the respective figures are 33.6 cu. ft. per lb. and 29.6 cu. ft. per lb. In each case the integrated particle velocity gives a greater volume change than the direct measurement of the radius by 8 and 13 percent, respectively. The error in the radius formula (36) is of the order of 2 percent, which could amount to an 8 percent error in the volume. The error in the double integration in Eq. (35) is of the order of 5 percent, because of base line inaccuracies, etc. (A base line shift of about 5 lb./in.^{2} in the pressure-time curve would

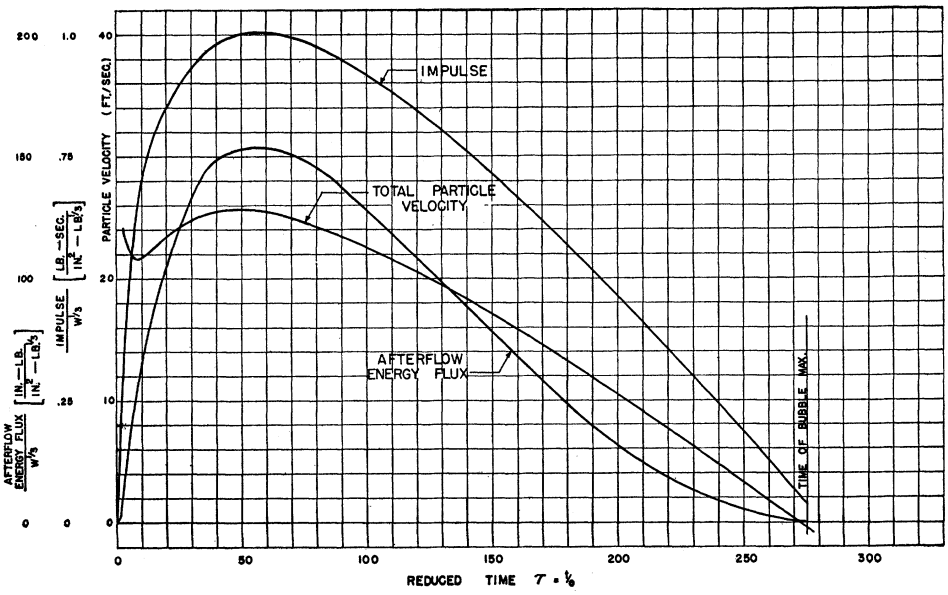

FIG. 9. Afterflow energy flux, impulse, and total particle velocity *versus* time to instant of first bubble maximum. Explosive: TNT; charge depth: 250 ft.; distance from center of charge: $R = W^{1/3}/0.352$; θ = time constant of initial shock-wave decay.

make the discrepancy in the volume almost negligible, while it would not seriously affect the impulse and afterflow energies, and a base line error of this magnitude could easily be present.) For these reasons it is impossible to say whether the discrepancy is due to inaccuracies in interpreting the experimental results or to inadequacy of the acoustic approximation.

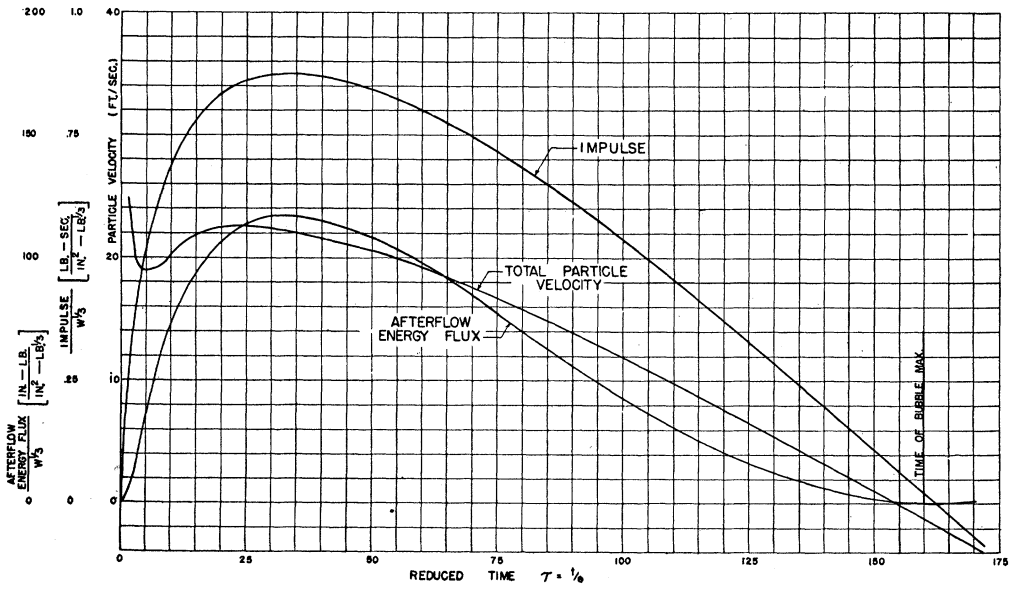

FIG. 10. Afterflow energy flux, impulse, and total particle velocity *versus* time to instant of first bubble maximum. Explosive: TNT; charge depth: 500 ft.; distance from center of charge: $R = W^{1/3}/0.352$; θ = time constant of initial shock-wave decay.

VI. IMPULSE AND ENERGY FLUX ASSOCIATED WITH THE BUBBLE PULSES

20

The bubble pulses have been defined as those parts of the pressure-time curve lying between times of successive bubble maxima. In practice, the times of bubble maxima are taken to be halfway between successive pressure peaks. This assumes that the time of expansion of the bubble is equal to the time of collapse. According to the theory of the bubble phenomenon,[7] the period (or half-period) is dependent on the amount of energy available for the oscillation. Since the bubble is continually radiating acoustic energy, the bubble expansion has more energy associated with it, and therefore actually lasts longer than the following contraction. Our approximation can be justified, however, because most of the radiation occurs in a relatively short length of time near the bubble minimum, and during the major portion of a cycle the bubble has nearly constant energy. The difference between the time of expansion and contraction should therefore be very small.

Composite curves of the first two bubble pulses from the series of measurements reported in reference (2) are reproduced in Fig. 11. The particular composites shown are for a depth of 500 ft. and $W^{\frac{1}{3}}/R$ equal to 0.352, the gauges being positioned to the side of the cylindrical charges used. The time scale has been reduced by the cube root of the charge size, thus:

$$z=t/W^{\frac{1}{3}}. \tag{37}$$

21

As in the case of the shock wave, it is possible to determine the nature of the net impulse delivered by a bubble pulse from theoretical considerations. At the time of a bubble maximum the following condition holds at the bubble surface:

$$u_M=0=\frac{\Delta P_M}{\rho_0 C_0}+\frac{1}{\rho_0 A_M}\int_0^{t_M}\Delta p\,dt, \tag{38}$$

where ΔP_M is the pressure in the gas bubble. The impulse as measured at A_M would therefore be:

$$I_{AM}=-(A_M\Delta P_M/C_0). \tag{39}$$

The impulse varies inversely as the radius (allowing for the time lag due to finite velocity of propagation), so that the impulse at radius R would be

$$I_R=-(A_M^2\Delta P_M/RC_0). \tag{40}$$

The incremental impulse delivered at a radius R_1 between the times of first and second bubble maxima would therefore be

$$\Delta I_R=(-A_{M2}^2\Delta P_{M2}/RC_0)-(-A_{M1}^2\Delta P_{M1}/RC_0). \tag{41}$$

The terms in parentheses are inherently small and positive since the ΔP_M's are small and negative. The first term is smaller than the second in magnitude because both A_{M2} and ΔP_{M2} are smaller than the corresponding quantities in the second term. ΔI_R, which is the net impulse delivered between the first and second bubble maxima, should therefore be small and negative. The same statement is, of course, true for the second and succeeding bubble pulses. The negative impulses delivered in this manner should ultimately cancel the net positive impulse delivered by the shock wave (see Section 16).

This treatment neglects the finite amplitude of the wave and other effects such as turbulence and migration of the bubble. The effect of these factors on the impulse is difficult to ascertain, but it is believed that the results of the above discussion are in any case qualitatively correct.

Integrations of Fig. 11 show that the positive impulse delivered by the first bubble pulse is 1.076-lb. sec./in.^{2} lb.$^{\frac{1}{3}}$, while the net impulse for the whole pulse is +0.106-lb. sec./in.^{2} lb.$^{\frac{1}{3}}$. Although the net impulse appears to be positive in contradiction to Eq. (41), a base line shift of the order of 5 lb./in.^{2} in Fig. 11 could make the impulse come out zero or even negative. This is the order of magnitude of the error in originally determining the base line on the photographic records.

If the net volume flow from the time of first bubble maximum to second bubble maximum is calculated from Eq. (35),

$$\Delta V=\frac{4\pi R}{\rho_0}\int_{t_{M_1}}^{t_{M_2}}\left[\int_0^t \Delta p\,dt\right]dt, \tag{35}$$

[7] Bernard Friedman, *Theory of Underwater Explosion Bubbles*, Report IMM-NYU 166, Inst. for Math. and Mech., New York University, September 1947.

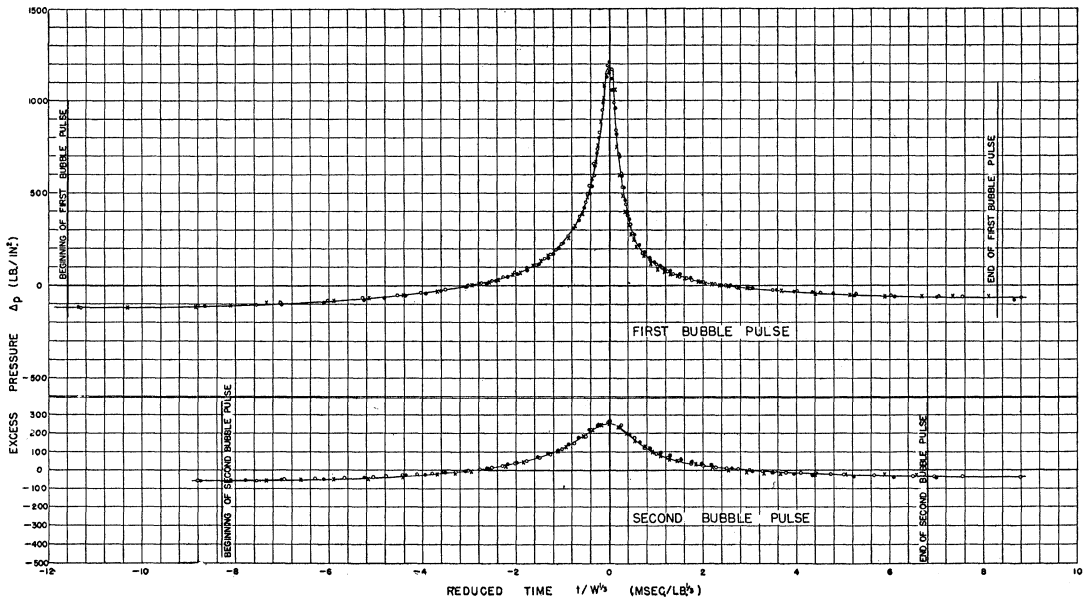

FIG. 11. Composite pressure-time curves for first and second bubble pulses. Explosive: TNT; charge depth: 500 ft.; distance from center of charge: $R=W^{\frac{1}{3}}/0.352$. (Based on measurements cited in reference 2.) Legend: ⊙ 0.5-lb. charges. × 2.5-lb. charges. ● 12.0-lb. charges.

it is found, using the curve of Fig. 11, that the net flow is 9.7 cu. ft. per lb. *toward* the bubble. The ratio of the volume of the bubble at its second maximum to its volume at first maximum should therefore be

$$(17.0-9.7/17.0)=0.43,$$

since the volume of 17.0 cu. ft. was found in Section 19 to be the total outward flow up to the time $t=t_{M1}$.

As in Section 19, we have at our disposal an equation giving the second bubble maximum in terms of the charge size and the depth:

$$A_{M2}=J_2(W/Z_0)^{\frac{1}{3}}, \tag{42}$$

where $J_2=8.5$.

The ratio of the first and second maximum volumes as obtained from direct bubble radius measurement is, therefore,

$$(A_{M2}/A_{M1})^3=(J_2/J_1)^3=0.31.$$

This ratio is considerably lower than the value of 0.43 given above by Eq. (35), but the discrepancy is in the direction of the same type of base line error that probably caused the net impulse to be positive. In this case the effect would be somewhat exaggerated because of the cumulative effect of base line error upon the integration.

The impulse of the second bubble pulse will not be considered as the error in the base line in that region is excessive.

22

The radiated energy flux for the first bubble pulse is given by the equation

$$F_{R1}=\frac{1}{\rho_0 C_0}\int_{t_{M_1}}^{t_{M_2}}(\Delta p)^2 dt. \tag{43}$$

Integration of the energy flux from the composite of Fig. 11, yields

$F_{R1}/W^{\frac{1}{3}}=139$(in.-lb./in.^{2} lb.$^{\frac{1}{3}}$) (at $R=W^{\frac{1}{3}}/0.352$)

and

$$E_{R1}/W=121\text{(cal./g)}.$$

Similarly, for the second bubble pulse

$F_{R2}/W^{\frac{1}{3}}=16.8$(in.-lb./in.^{2} lb.$^{\frac{1}{3}}$) (at $R=W^{\frac{1}{3}}/0.352$),

$E_{R2}/W=14.7$(cal./g).

The error in the energy flux of bubble pulses caused by error in the base line is very small

TABLE I. Reported detonation energies of TNT.

ΔH cal./g	Source
840	*Bericht über die Arbeitstagung Unterwassersprengwesen, Veranstaltet von der Amtsgruppe Mar Rust*/FEP im OKM am 28/29 Oktober 1943 im Harnackhaus im Berlin (experimental)
880	G. I. Taylor, *The Vertical Motion of a Spherical Bubble and the Pressure Surrounding It*, TMB 510, August 1943
950	G. D. Clift and B. T. Federoff, *A Manual for Explosives Laboratories* (Lefax, Inc., Philadelphia, 1942). This value seems to have been obtained from Soukharevsky and Pershakoff, Explosives, Moscow, 1932
1060	Private communication from S. R. Brinkley to W. D. Kennedy (theoretical)

TABLE II. Energy partition at time of first bubble maximum (W=charge weight in lb.; R=distance in ft.).

Acoustic energy flowing past $R=W^{\frac{1}{3}}/0.352$	275 cal./g
Energy dissipated at the shock front during propagation up to $R=W^{\frac{1}{3}}/0.352$ (calculated in Section 13)	200
Unaccounted for	95
Total energy associated with emission of shock wave (1050−480)	570
Potential energy stored in water at first bubble maximum as calculated from measured maximum bubble radius	385
Internal energy of gaseous products (referred to infinite adiabatic expansion: (480−385)	95
	1050

because of the fact that the calculated energy flux is near a minimum with respect to a base line shift. In this case an error of 10 lb./in.^{2} in the base line would cause less than 2 percent error in the energy, while it would cause a very large error in the impulse.

VII. PARTITION OF ENERGY IN AN UNDERWATER EXPLOSION

23. Energy of Detonation

At the present time there seems to be a lack of precise knowledge concerning the quantity of energy released in the detonation of various explosives. A wide range of values is quoted in the literature, and it is not always possible to ascertain the original source of the data. A summary of such results is given in Table I. Detonation energy is defined as the enthalpy change, ΔH, in calories per gram, with final products reduced to standard conditions.

In the theory of the gas bubble oscillation[7] it is customary to use as a zero energy reference the state of infinite adiabatic expansion of the product gases. Since it is our purpose to include bubble phenomena in the discussion of energy partition, it will be more convenient to adopt this reference rather than the standard state usually used for ΔH. The order of magnitude of the internal energy of the products at standard conditions (relative to infinite adiabatic expansion) is 100 cal./g, and this quantity should be added to the values given in Table I.

For purposes of further discussion, we shall arbitrarily adopt the value of 950 cal./g as the detonation energy of TNT, giving 1050 cal./g as the approximate detonation energy relative to infinite adiabatic expansion of the products. The uncertainty in this figure is at least of the order of ± 10 percent.

24. The Shock Wave

It is known that the total energy associated with the gas bubble at its first maximum is approximately 480 cal./g.[2] Of this quantity, 385 cal./g are stored as potential energy because of the formation of the cavity in the water, while the remainder is in the form of internal energy of the gaseous products (referred to an infinite adiabatic expansion). The value of the potential energy stored in the water is based on the experimental maximum radius as given by Eq. (36).

The net energy lost by the bubble up to the time of the first maximum is therefore 1050 minus 480, or about 570 cal./g.

The partition of this energy has been discussed in previous chapters and is summarized in Table II.

The unaccounted term should comprise losses resulting from turbulence, viscosity, conduction, etc. It should be noted that the magnitude of

TABLE III. Successive periods of bubble oscillation (TNT charges in free water)* at a depth of 500 ft.

$T_1/W^{\frac{1}{3}}=23.2$ millisec./lb.$^{\frac{1}{3}}$
$T_2/W^{\frac{1}{3}}=16.7$
$T_3/W^{\frac{1}{3}}=13.5$

* See reference 2.

TABLE IV. Energy partition at time of second bubble maximum.

Acoustic radiation in first bubble pulse	120 cal./g
Potential energy in the water at time of second bubble maximum based on measured maximum radius	120
Internal energy of gas at second bubble maximum: (B_2-120)	60
Unaccounted for	180
Total energy associated with first maximum (B_1)	480 cal./g
Total loss during emission of first pulse (180+120)	300
Energy left for second pulse (B_2)	180

TABLE V. Energy partition at time of third bubble maximum.

Acoustic radiation in second bubble pulse	15 cal./g
Potential energy in the water at time of third bubble maximum	55
Internal energy of gas at third bubble maximum: (B_3-55)	40
Unaccounted for	70
Total energy associated with second bubble maximum (B_2)	180 cal./g
Total loss during emission of second pulse =70+15	85
Energy left for succeeding pulses (B_3)	95

this portion (95 cal./g) is much smaller than the combined uncertainty in the detonation energy and in the energy dissipated at the shock front, and therefore even its order of magnitude is in doubt.

25. The Bubble Pulses

From the theory of the bubble pulsation it is known that the period is proportional to the cube root of the total energy associated with the oscillation as defined in Section 24. Since the periods of successive oscillations decrease progressively, it is evident that energy is lost between successive bubble maxima. Using the cube root law stated above, it is seen that the energy left after the emission of a bubble pulse is given by

$$B_{n+1}=B_n(T_{n+1}/T_n)^3, \qquad (44)$$

where B_n=total energy associated with the nth oscillation and T_n=period of nth oscillation.

The necessary period data[2] are summarized in Table III.

Using Eq. (44), the data of Table III, and the maximum radius data quoted in Sections 21 and 22, we obtain the energy partition for the first and second bubble pulses as given in Tables IV and V.

Since the total energy associated with an oscillation and the energy of acoustic radiation are both known to within ±3 percent, it is important to note the magnitude of the unaccounted terms in Tables IV and V.

A summary of energy partition data is given in Table VI. It is seen from Table VI that less than half the detonation energy is to be found in waves of compression, while somewhat more than half is lost in dissipative processes.

It is difficult to ascribe any appreciable portion of the unaccounted 345 cal./g to dissipation similar to that which was computed for the shock front. Figure 11 shows the pressure pulses to rise relatively slowly with time, and the resulting process should be very nearly isentropic on both compression and expansion. Furthermore the second pulse rises very much more slowly than the first, and yet the unaccounted portion in this pulse is an even greater *fraction* of the total energy loss than is the case in the first pulse.

Because of the shortness of the time intervals during which temperature and pressure in the gas bubble are high, it is doubtful that losses of such magnitude could be attributed to conduction or radiation of heat.

We conclude, therefore, that the unaccounted for energy losses are associated with some combination of the following factors:

(i) turbulence induced in the water surrounding the bubble,

(ii) chemical or physical changes in the gaseous products,

(iii) actual loss of gaseous products in the form of small bubbles in the water, perhaps due to high degree of turbulence at the periphery of the gas globe.

TABLE VI. Summary of energy partition tables.

Total acoustic radiation (through emission of second bubble pulse) at $R=W^{\frac{1}{3}}/0.352$	410 cal./g
Shock front dissipation up to $R=W^{\frac{1}{3}}/0.352$	200
Unaccounted losses	345
Total energy left at third bubble maximum	95

APPENDIX I

Summary of Notation

p = absolute pressure at any point as a function of time
P_0 = absolute hydrostatic pressure
Δp = excess pressure as a function of time $(p-P_0)$
P_m = excess peak pressure of an exponentially decaying shock wave
ΔP_s = excess pressure at any shock front
v = specific volume of the fluid at pressure p
ρ = density of the fluid $(\rho=1/v)$
E = total energy flow through a spherical surface
F = energy flux (energy flow per unit area of a spherical surface)
R = radial distance
A = radius of the gas bubble
t = time measured from instant of incidence of the pressure wave
u = radial particle velocity relative to the unperturbed fluid
U = shock front propagation velocity
C_0 = sound velocity $(C_0=(\partial P/\partial\rho)_{s_0}^{\frac{1}{2}})$
$\Delta\eta$ = internal energy increment of a unit mass of fluid relative to the initially unperturbed state
ΔH = enthalpy increment of a unit mass of fluid relative to the initially unperturbed state $(\Delta H=\Delta\eta+\Delta(pv))$
h = dissipated portion of the enthalpy increment ΔH, per unit mass of fluid
S = entropy per unit mass of fluid
κ = bulk modulus of the fluid $(\kappa=\rho_0 C_0^2)$
θ = time constant of initial exponential decay of shock wave
$B(S)$ = characteristic pressure parameter of the modified adiabatic Tait equation of state
n = exponent of Tait equation of state
x = reduced radius $(x=R/W^{\frac{1}{3}})$
I = impulse delivered—the time integral of the pressure
τ = reduced time defined by $\tau=t/\theta$
z = reduced time defined by $z=t/W^{\frac{1}{3}}$
T_n = period of nth oscillation, measured between successive pressure peaks
B_n = total energy associated with the nth oscillation.

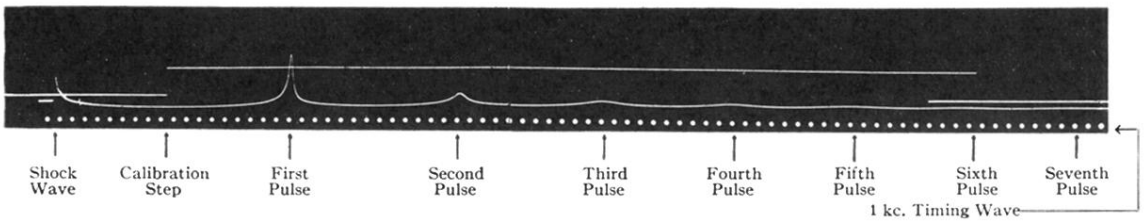

FIG. 1. Pressure-time record showing shock wave and bubble pulses. Charge: 0.505-lb. TNT; gauge dist: 2.25 ft.; depth: 500 ft.